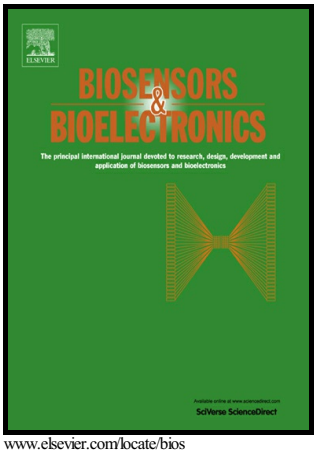

www.elsevier.com/locate/bios

A rapid and visual aptasensor for lipopolysaccharide detection based on the bulb-like triplex turn-on switch coupled with HCR-HRP nanostructures

Wentao Xu, Jingjing Tian, Xiangli Shao, Longjiao Zhu, Kunlun Huang, Yunbo Luo

PII: S0956-5663(16)31008-9
DOI: http://dx.doi.org/10.1016/j.bios.2016.10.012
Reference: BIOS9234

To appear in: *Biosensors and Bioelectronic*

Received date: 25 August 2016
Revised date: 24 September 2016
Accepted date: 4 October 2016

Cite this article as: Wentao Xu, Jingjing Tian, Xiangli Shao, Longjiao Zhu Kunlun Huang and Yunbo Luo, A rapid and visual aptasensor for lipopolysaccharide detection based on the bulb-like triplex turn-on switch coupled with HCR-HRP nanostructures, *Biosensors and Bioelectronic* http://dx.doi.org/10.1016/j.bios.2016.10.012

A rapid and visual aptasensor for lipopolysaccharide detection based on the bulb-like triplex turn-on switch coupled with HCR-HRP nanostructures

Wentao Xu[1,2], Jingjing Tian[2], Xiangli Shao[1], Longjiao Zhu[2], Kunlun Huang[1,2], Yunbo Luo[1*]

[1]Beijing Advanced Innovation Center for Food Nutrition and Human Health, College of Food Science & Nutritional Engineering, China Agricultural University, Beijing 100083, China

[2]Beijing Laboratory for Food Quality and Safety, College of Food Science and Nutritional Engineering, China Agricultural University, Beijing 100083, China

[*]To whom correspondence should be addressed. Tel./Fax: +86 010 62736479; lyb@cau.edu.cn

Abstract

For previously reported aptasensor, the sensitivity and selectivity of aptamers to targets were often suppressed due to the reporter label of single-stranded molecular beacon or hindrance of the duplex DNA strand displacement. To solve the affinity declining of aptamers showed in traditional way and realize on-site rapid detection of Lipopolysaccharides (LPS), we developed an ingenious structure-switching aptasensor based on the bulb-like triplex turn-on switch (BTTS) as the effective molecular recognition and signal transduction element and streptavidin-horseradish peroxidase modified hybridization chain reaction (HCR-HRP) nanocomposites as the signal amplifier and signal report element. In the presence of LPS, the bulb-like LPS-aptamer (BLA) and LPS formed the LPS/aptamer complex, while the BTTS disassembled and

liberated the dissociative bridge probes (BP) to achieve molecular recognition and signal transduction. Immobilized BP, captured by immobilized capture probes (CP), triggered hybridization chain reactions (HCR) to amplify the switching signal, and the HCR products were then modified with streptavidin-horseradish peroxidase (SA-HRP) to form HCR-HRP nanostructures to output colorimetric signals. In less than four hours, the proposed biosensor showed a detection limit of 50 pg/mL of LPS quantitatively with the portable spectrophotometer and the observation limit of 20 ng/mL semi-quantitatively with the naked eye, opening up new opportunities for LPS detection in future clinical diagnosis, food security and environment monitoring.

Keywords: visual, aptasensor, Lipopolysaccharides, DNA triplex, hybridization chain reaction.

Introduction

Lipopolysaccharides (LPS), also termed endotoxins, are the major component of the outer membrane of Gram-negative bacteria(Gutsmann et al. 2007; Li et al. 2004; Therisod et al. 2001), which cause hemorrhagic colitis(Shen et al. 2011), blood clotting(Kotani et al. 1985), pyrogenic reactions and septic shock(Ding et al. 2007; Murai et al. 1987). To keep pace with expectations in the clinical diagnosis, food security and environment monitoring(Kim et al. 2005; Rapson 1988), limulus amebocyte lysate (LAL) (Pedersen et al. 1994), silver staining techniques and immunological detection methods were established(Kittelberger and Hilbink 1993; Lei and Morrison 1988). However, there still exists an urgent need for more flexible, yet sen-

sitive, quantitative sensing techniques for LPS detection due to false positive interference(Foto et al. 2004), environmental risk addition and vulnerability to the harsh conditions of traditional methods(Simoons-Smit et al. 1996; Zhu et al. 2012).

Among the newly developed sensors, aptamer-based biosensors have become particularly attractive since the LPS binding aptamer was selected by the Kim group in 2012(Kim et al. 2012; Su et al. 2012; Xie et al. 2016). Aptamers, fragments of short oligonucleotides, were generated from an *in vitro* selection process termed systematic evolution of ligands via exponential enrichment (SELEX) (Ellington and Szostak 1990; Tuerk and Gold 1990). As the target recognition element, aptamers showed outstanding advantages of high affinity, impressive target selectivity, thermal tolerance and ease of chemical synthesis compared to antibodies(Liu et al. 2009). To design an aptasensor, two types of conformational alteration strategies are commonly applied during the aptamer-target binding event. One is the single-stranded molecular beacon strategy. Structural alteration of the molecular beacon, which consisted of aptamers labeled with different signal reporters, generated fluorescent or electrochemical signals (Hamaguchi et al. 2001; Li et al. 2002; Tang et al. 2008). Nevertheless, signal reporter labels evidently reduce the sensitivity and selectivity of aptamers to targets (Beyer et al. 2005; Jhaveri et al. 2000). The other strategy is the duplex DNA structure-switching strategy in which the complementary strand hybridized with the aptamer strand via Watson-Crick base pairing(Li et al. 2007; Nutiu and Li 2003). Upon target introduction, the aptamer combined with the target, displacing the complementary strand. However, the length of hybridization segment of the two strands impacted

the recognition to the target, lowering the affinity of aptamers(Li and Ho 2008).

Interestingly, hybridization chain reactions (HCR), which generated linear polymeric nanostructures initiated by self-assembly of short oligonucleotides through a cross-opening process, has attracted increasing attention in molecular biology and DNA diagnostics, due to the characteristic of non-enzymatic signal amplification(Filippov et al. 2009; Tang et al. 2012). Inspiringly, biotinylated short oligonucleotides formed polymeric nanostructures. Upon streptavidin modified horse radish peroxidase (SA-HRP) addition, HCR nanostructures were crosslinked to HCR-HRP nanocomposites via biotin-streptavidin linkage, serving as a signal amplifier and signal conversion element.

Herein, we developed a novel structure-switching analytical method for LPS detection based on the bulb-like triplex turn-on switch (BTTS) as a selective molecular recognition and signal transduction element and streptavidin-horseradish peroxidase modified hybridization chain reaction (HCR-HRP) nanostructures as effective signal amplifier and signal report element. As illustrated in Fig. 1, BTTS was designed as bulb-like and was composed of a bulb-like LPS-aptamer (BLA) in the center to capture LPS from *E. coli O111:B4* flanked by mirror sequences to hybridize with the bridge probe (BP) to form a triplex nucleic acid stem by Watson-Crick base pairing and Hoogsteen base pairing. As the molecular recognition element, the nudity of the bulb-like aptamers promoted effective binding to LPS. Compare with two conformational alteration strategies, neither signal reporter labels nor hybridization of double strands interfere the sensitivity and affinity of aptamers to targets. When LPS was introduced,

BTTS turned on, which means that the triplex nucleic acid stem disassembled and liberated LPS-combined aptamers and dissociative BP. After dissociative BP was anchored by an immobilized capture probe (CP) on the surface, Biotin-H_1 and Biotin-H_2 were initiated to proceed HCR via cross-opening linkage. Upon SA-HRP addition, HCR-HRP nanocomposites were formed, serving as the signal amplifier and signal report element, which catalyzed hydrogen peroxide (H_2O_2) via TMB to generate an obvious green color and turned yellow after sulfuric acid termination with optical absorption at 450 nm. The chromogenic output was able to be semiquantitatively monitored by the naked eye and quantitatively inspected by a portable spectrophotometer. In our design, turning on the BTTS was equivalent to the occurrence of the aptamer-target binding event, converting LPS content to visual output accompanied by the generation and amplification of the detection signal. Because the BTTS and immobilized CP could be prepared in advance, the actual total detection time, including the LPS sample introduction for 0.5 h, BP anchoring for 1 h, and the generation and amplification of the detection signal for less than 2 h (composed of HCR for 1 h, the formation of HCR-HRP nanocomposites for 40 min and chromogenic reaction via TMB for 5 min), was less than 4h, indicating great promise for on-site rapid analysis.

(Here Fig. 1)

Material and methods

Reagents and Apparatus

All synthetic DNA sequences in Table S1 were synthesized at Invitrogen (Life Technologies, Beijing, China). High binding polystyrene 96-welll microplate was pur-

chased from Costar (NY, USA). Streptavidin (SA), D-mannose, peptidoglycan from *S. aureus*, hemoglobin (Hb), glucose, human serum albumin (HSA), bovine serum albumin (BSA), streptavidin-horseradish peroxidase (SA-HRP), LPS from *E. coli O55:B5*, LPS from *E. coli O111:B4*, biotinylated HRP were obtained from Sigma Aldrich Chemical Co. (St. Louis, MO, USA). Tetramethylbenzidine (TMB) coloring solution was purchased from Biyuntian Co. Ltd (Beijing, China). The coating buffer was carbonate buffer solution (CBS, 15 mM Na_2CO_3, 35 mM $NaHCO_3$, pH 9.6). The working buffer was PBS buffer containing 20 mM KCl, 2.5 mM $MgCl_2$, at pH 6.2. The washing buffer consisted of 0.15 M NaCl, 10 mM K_2HPO_4, 1 mM NaH_2PO_4, 0.05% Tween20, at pH 7.4. Ultrapure water used throughout was obtained from a Milli-Q water purifying system (resistivity ≥ 18.2 MΩ cm^{-1}, Milli-Q, Millipore). Other chemicals were of analytical grade and were used without further purification.

Gel electrophoresis was conducted on a Molecular Imager Gel Doc XR (Bio-Rad, Canada). Visual measurements were carried out with a portable spectrophotometer (NS810, Shenzhen 3nh Technology Co., Ltd). The UV−vis absorption spectra were recorded with a UV-2550 spectrophotometer (Shimadzu, Japan). The transmission electron micrograph (TEM) was performed on a JEOL JEM-1400 Transmission electron micrograph (Germany).

Preparation of Immobilized CP

The immobilized CP is shown in Fig. 1. Briefly, 100 μL of SA (6 μg/mL) in the coat-

ing buffer was added to each well of the high binding polystyrene 96-welll microplate and incubated for 2 h at 37 °C, which worked as a cross-linking agent. After the wells were washed three times with 250 μL wash buffer, each coated well was blocked with 200 μL of 1% BSA at 37 °C for 2 h to minimize non-specific adsorption. After washing three times, 100 μL of biotinylated CP solution (360 nM) was dropped into each well with incubation at 37 °C for 1 h. To test the SA coating effect, biotinylated HRP was displaced with biotinylated CP, catalyzing TMB to an output visual signal.

Fabrication of the BTTS Aptasensor

First, 35 μL of BLA stock solution (10 μM) and 35 μL of BP stock solution (10 μM) were mixed in 930 μL working buffer and incubated at 37 °C for 1 h, obtaining the bulb-like triplex turn-on switch (BTTS). Then, 20 μL of LPS solution with different concentrations were mixed with the above reaction system and incubated at 37 °C for 30 min. Finally, the solution containing different concentrations of released BP was anchored by immobilized CP via Waston-Crick base pairing for 1 h at 30 °C. Before further use, each well was washed three times. To conform the structure switching of BTTS, HPLC was conducted.

HPLC-DAD analysis

Conditions for DNA analysis followed the description by Wilde et al. with some modifications. HPLC analyses were performed on an Agilent 1100 HPLC system together with a diode array detector (DAD) (Wilde et al. 2003). A TSK gel DNA-NPR (4.6 mm i.d.×7.5 cm, Tosoh, Japan) was employed. DNA samples were separated by buffer A (20 mM Tris, pH 9.0) and buffer B (1 M NaCl in 20 mM Tris, pH 9.0) according to

the following gradient: 25-45% B in 0-0.13 min, 45–50% B in 0.13–4 min, 50–64% B in 4–25 min, 25% B in 25.1–35 min. The flow rate was 0.4 mL/min with an injection volume of 10 μL. DNA elution was monitored by UV absorbance at 260 nm. All chromatography was carried out at 35℃.

HCR-HRP signal output

Biotin-H_1 and Biotin-H_2 were heated to 95 °C for 5 min and then cooled to room temperature for 1 h before use. Each above prepared well was mixed with 1 μM Biotin-H_1 and 1 μM Biotin-H_2 in 100 μL of HCR buffer (8 mM Na_2HPO_4, 2.5 mM NaH_2PO_4, 0.15 M NaCl, 2 mM $MgCl_2$, pH 7.4) and incubated for 37 °C for 1 h. After washing, 100 μL of SA-HRP was added to the buffer and shaken at 37 °C for 40 min. After washing three times, each well was supplemented with 100 μL TMB coloring solution, incubated at room temperature away from light for 5 min and added to 50 uL H_2SO_4 (2 M) to terminate chromogenic reactions, monitoring the optical intensity of 450 nm (OD_{450}) with a portable spectrophotometer (NS810, Shenzhen 3nh Technology Co., Ltd). HCR nanostructures were identified by agarose gel electrophoresis and the transmission electron micrograph (Liu et al. 2008).

Agarose Gel Electrophoresis

HCR nanostructures were initiated by definite concentrations of BP, 1 μM Biotin-H_1 and 1 μM Biotin-H_2, respectively. Then, 10 μL of each product were subjected to gel electrophoresis in 2% agarose gels at 130 V for 25 min and then stained with ethidium bromide. Images were documented by the Gel Doc UV 91 system (Bio-Rad, USA).

Results and Discussion

Optimization of Immobilized CP

Given that capture probes (CP) was immobilized onto the surface via biotin-streptavidin interaction, the concentration of SA and biotinylated CP were optimized. To achieve optimally sensitive signal output, optimal density at 450 (OD_{450}) was monitored as an evaluation index. In Fig. 2A, with the concentration of SA ranging from 1.0 to 8.0 μg/mL, the plot of OD_{450} presented a bell-shaped curve with a maximal signal at 6 μg/mL SA, presumably due to the stereo-hindrance effect. Small amounts of SA could not capture enough biotinylated substrate strand, while excess SA was attributed to steric hindrance, reducing the binding with the strand(Bouças et al. 2008). In Fig. 2B, the value of the detection signal gradually inclined until it reached a plateau at 360 nM from a low dose to high dose, mainly because the combination of streptavidin with biotin conformed to the molar ratio of one to four (SA: 6 μg/mL ≈ 90 nM) (Lee et al. 1994; Weber et al. 1989).

Characterization and Optimization of the BTTS Aptasensor

As presented in Fig. 1, BTTS was designed as bulb-like, with the aptamer in the center to recognize and to capture LPS from *E. coli O111:B4* flanked by mirror sequences to hybridize with BP to form triplex nucleic acid stems via Watson-Crick base pairing ("-") and Hoogsteen base pairing ("•"). Upon LPS introduction, the binding of BLA and LPS led to the formation of a structured LPS/aptamer complex. Meanwhile, the triplex nucleic acid stem disassembled and liberated LPS-combined aptamers and dissociative BP. Compared with two conformational alteration strategies,

the nudity of the bulb-like aptamers promoted effective binding to LPS due to the existence of neither signal reporter labels nor hybridization of double strands, which interfere the sensitivity and affinity of aptamers to targets. The turning on of the BTTS was equivalent to the occurrence of the aptamer-target binding event, converting LPS content to visual output accompanied by the generation and amplification of the detection signal.

The conformational transformation of BTTS structure was based on the equilibrium between the formation of triplex nucleic acid stem composed of BLA and BP and the deconstruction of the triplex stem, which directly influenced the efficiency of the target/aptamer-binding event and signal output(Zheng et al. 2014; Zheng et al. 2011). Recognizing that the key of the equilibrium lay in the flanked mirror sequences, we optimized the length of the flanked mirror sequences of BLA by forming T-A•T and C-G•C^+ base triplets and by monitoring OD_{450} as an evaluation index to obtain sensitive signal output (Table S1) (Dohno et al. 2002). According to the length of LPS-aptamer, BLA1 to BLA4 were designed as 7, 9, 11, 13 base triplexes, respectively. As shown in Fig. 3A, BLA3 presented optimal signal variation before and after LPS addition. Presumably, when the length of flanked mirror sequences was short, the integration of triplex nucleic acid stems was unstable and even did not occur, giving rise to little signal enhancement before and after the introduction of LPS. Increasing the length, triplex nucleic acid stem was formed. Upon LPS addition, the triplex stem deconstructed and liberated BP to enhance the signal response. However, once the triplex-stem length was increased to 13 base triplexes, the BTTS structure was too stable

to disassemble, even in presence of a high concentration of LPS.

The formation of triplex nucleic acid stems depended on Watson-Crick and Hoogsteen base pairing, and the stability of the Hoogsteen base pairing was pH dependent even weak acid environment accelerated the formation of Hoogsteen base pairing (Karympalis et al. 2004; Plum 1997). Inspired by this, the influence of the working buffer pH on the formation of BTTS was studied. The working buffer pH was selected as 5.0, 6.0, 7.0, 8.0. As illustrated in Fig. 3B, pH 6.0 was optimal. That was mainly because the amino group of cytosines in the C-G•C^+ base triplet easily realized protonation to form Hoogsteen base pairing in an acid environment, while neutral working buffer cytosines could not protonate, leading to Hoogsteen base pairing and even triplex stems unable to form. Interestingly, BTTS aptasensor output had weak signal enhancement at pH 5.0. That was presumably due to the low affinity of BLA to recognize and combine with LPS.

Since the BTTS structure was composed of the bulb-like BLA and the BP to form a triplex nucleic acid stem, the ratio of BLA versus BP was optimized by monitoring OD_{450} as an evaluation index to achieve optimally sensitive signal output. In theory, the ratio of BLA versus BP 1.0 was optimal for the formation of a triplex nucleic acid stem. But in actual experiment, a little excessive one in two ingredients would be in favor of the combination of two ingredients. However, more BLA was likely to produce false-negative errors due to LPS combining with spare BLA consumed by BP. While more BP was likely to produce false-positive errors due to spare BP anchored by CP in the well. So we selected the ratios 0.9, 1.0, 1.1 and 1.2 for optimization. As

shown in Fig. 3C, when the ratio of BLA versus BP was 0.9 to 1.0, the value of the background was relatively high, primarily due to slightly excess BP contributing to false positives. When the ratio increased from one to one to one to one point two, the signal enhancement became lower and lower on account of excess BLA consuming LPS in the detection system. Therefore, the optimal ratio of BLA versus BP was one to one.

Anion exchange chromatography is a widely used technique for separating negatively charged DNA molecules. The TSK gel DNA-NPR column is a polymer-based anion exchange column designed for improved resolution of DNA molecules over a wide molecular weight range. The capability of the TSK gel DNA-NPR column to separate both high and low molecular weight DNA fragments has been demonstrated. Given that, the formation and disassembly of BTTS was analyzed with the DNA-NPR column, which was based on the variation of the charge distribution of BLA. In Fig. 4, the typical elution profiles of the negative control of the BLA3 and the BTTS composed of BLA3 and BP before and after the addition of LPS, respectively, are shown. Fig. 4A shows the relatively high response value at the retention time of 15.93 min with the corresponding peak area of 242.7 and the retention time of 16.105 min with a peak area of 242.7, which indicated that the chromatographic peak resulted from the BLA3 single strand. Whereas the BTTS had a small response at 15.25 min and 16.438 min with corresponding peak areas of 30.8 and 43.6, respectively, there was no new chromatographic peak, as shown in Fig. 4B, which suggested that the formation of BTTS consumed some BLA3, and the positive charge of the BTTS led to the absence

of a new chromatographic peak due to the positive charge of the protonation C-G•C+ base triplet. Upon the introduction of LPS in Fig. 4C, there was no response at 15 min and 16 min, yet a new chromatographic peak appeared at the retention time of 5.763 with corresponding peak area of 406.3, which manifested the chromatographic peak derived from the LPS/BLA3 complex and the disassembly of the BTTS. Based on these scientific data, we concluded that there was conformational change of BTTS before and after the addition of LPS.

Characterization of HCR-HRP Nanocomposites

Agarose gel electrophoresis was employed to characterize the HCR-HRP nanostructures. To initiate the cascade of hybridization, Biotin-H_1 and Biotin-H_2 were designed as hairpin structures labeled with a biotin group at the 5'-terminus (sequences are shown in Table S1). In the presence of BP, Biotin-H_1 was opened from the sticky end and paired with BP, undergoing an unbiased strand-displacement interaction. Immediately following this event, the newly released sticky end of the Biotin-H_1 hairpin hybridized with the Biotin-H_2 hairpin from its sticky end via a strand displacement reaction, generating new single-stranded linker sequences that were identical to BP. In this way, the opening of hairpins continued, accompanied by strand displacement reactions, until the formation of a long linear nanostructure labeled with biotin group. Upon SA-HRP addition, HCR-HRP nanocomposites were formed via biotin-streptavidin interactions. As proof-of-principle, HCR triggered by BP and Biotin-H_1 and Biotin-H_2 were examined by ethidium bromide (EB)-stained agarose gel

electrophoresis (Fig. 5A). In the absence of BP, HCR between Biotin-H_1 and Biotin-H_2 was inhibited, as shown in lane 4. However, emission bands of high-molecular weight nanostructures could be inspected in lanes 5−10, indicating how much higher the ratio of BP versus hairpins was and how much lower the molecular weights of the HCR nanostructures were. Therefore, the results suggested that a low concentration of BP was able to trigger HCR, and the optimal ratio of BP versus hairpins was one to ten. Considering the concentration of SA-HRP (Fig. 5B), the optical intensity at 450 nm went up until it reached a stable region in which the concentration of SA-HRP was more than 750 ng/mL, demonstrating the optimal dosage was 750 ng/mL avoid of dissipation. As shown in Fig.S1, OD_{450} of the HCR-based system was obviously higher than that of the non-HCR system, and the sensitivity was noticeably improved, clearly indicating that the signal amplification effect of HCR process, which was at least 4-fold greater than that in the non-HCR method.

In addition, transmission electron microscope (TEM) was further employed to observe the morphology of the assembled HCR-HRP nanostructures. From Fig.3S, morphology with helical nanocomposites was observed. The result suggested the successful formation of the HCR-HRP nanostructures.

Analytical Performance of BTTS Aptasensor for LPS Detection

By virtue of the optimal conditions, the sensitivity and quantitative range of the BTTS aptasensor were evaluated for the detection of a series of different concentrations of LPS from *E. coli O111:B4*. As shown in Fig. 6A, the plot of optical intensity at 450

nm versus the concentration of LPS displayed a good linear relationship in the range from 1 to 150 ng/mL with a regression equation expressed as y = 0.016x + 0.6226, and the correlation coefficient was 0.9981. The limitation of detection (LOD) was calculated to be 50 pg/mL in terms of the rule of three times the standard deviation over the blank response (Macdougall and Crummett 1980). Moreover, the analytical performances of different techniques for LPS analysis are summarized and the sensitivity of the BTTS aptasensor is competitive compared to these techniques (see Table S2), which should be attributed to the nudity of the aptamers and HCR-HRP nanostructures for signal amplification.

The specificity of the BTTS turn-on aptasensor was evaluated by challenging the system against other interfering agents; e.g., D-mannose, BSA, peptidoglycan from *S. aureus*, hemoglobin (Hb), glucose, human serum albumin (HSA) and LPS from *E.coli O55:B5*. As indicated in Fig. 6B, in contrast to significant responses observed for LPS and the mixture containing the above seven interferences, other agents showed very low interference to LPS detection. Such an excellent selectivity might be attributed to the high specificity of the aptamer of LPS from *E. coli O111:B4*. Hence, the developed BTTS turn-on aptasensor could be used for specific detection of LPS.

Analysis of LPS in Real Samples

To further elucidate the feasibility of the BTTS aptasensor for application, the recovery experiments, which employed the standard addition method based on drinking water and human serum as real samples, were performed. Non-contaminated com-

mercial bottled purified water, used as a drinking water sample, was purchased from the local supermarket. Rat serum samples were obtained from Supervision, Inspection & Testing Center of Genetically Modified Food Safety, MOA, (Beijing). Prior to use, the serum was obtained by centrifugation of clotted blood at 3000 rpm for 20 min and then collected and stored at －20 °C for further use. Then, the water samples and serum samples were each gently mixed with *E. coli O111:B4* LPS standard solution to obtain final LPS concentrations at three levels (5 ng/mL, 50 ng/mL, 100 ng/mL). After that, 10 μL of the real sample were mixed with 90 μL of the working buffer, and then the obtained 100 μL solution was treated using the same protocol as above for the LPS detection. As shown in Fig. S2, a color chart was designed to assist the qualitative analysis and semi-quantitative LOD of 20 ng/mL was clearly visualized by the naked eye. 50 ng/mL and 100 ng/mL of *E.coli O111:B4* LPS could be inspected by the naked eye semi-quantitatively. While 5 ng/mL of LPS could not be detected, since trace LPS could not be inspected by the naked eye below 20 ng/mL. In addition, real samples were also monitored according to the conventional enzyme-linked immunosorbent assay (ELISA) method. As shown in Table S3, the recoveries of LPS detected in the drinking water samples ranged from 95.2% to 98.2% and ranged from 96.6% to 104. 1% in the serum samples. The data obtained by our BTTS aptasensor exhibited good accordance with that calculated with the ELISA method, suggesting that our technique showed satisfactory accuracy for LPS detection in complicated samples.

Conclusion

In summary, we have developed a novel turn-on platform for the on-site rapid and visual analysis of LPS based on the structure-switching BTTS as a selective molecular

recognition and signal transduction element coupled with HCR-HRP nanostructures as the signal amplifiers and signal report elements. The liquid phase LPS-detection biosensor displayed several excellent features: (1) *The BTTS design*. In the BTTS, there were bulb-like LPS aptamers exposed in the center and flanked mirror sequences hybridizing with BP to form a triplex stem. As the molecular recognition element, the nudity of the bulb-like aptamers promoted remarkable recognition and binding to LPS compared with traditional strategies. Upon the addition of LPS, turning on the BTTS was equivalent to occurrence of the aptamer-target binding event, converting LPS content to visual output accompanied by the generation and amplification of a detection signal. (2) *Visualization*. As the signal amplifier and signal report element, HCR-HRP nanostructures could catalyze hydrogen peroxide (H_2O_2) via TMB, generating an obvious green color and turning yellow after sulfuric acid termination with optical absorption at 450 nm. The signal output could be semi-quantitatively observed with the observation limit of 20 ng/mL by the naked eye and quantitatively monitored with the LOD of 50 pg/mL by a portable spectrophotometer, demonstrating immense potential for on-site analysis. (3) *Sensitivity*, *selectivity* and *anti-interference*. Our proposed platform possesses outstanding sensitivity, selectivity and anti-interference, exhibiting a linear calibration from 1 to 150 ng/mL and displaying outstanding applicability for monitoring LPS in rat serum samples by virtue of the nudity of the BLA, which promotes effective binding to LPS and the signal amplification of HCR-HRP nanostructures. (4) *Rapidity*. Because the formation of BTTS and immobilized capture probe (CP) could be prepared in advance, the actual reaction time after the LPS sample introduction was less than 4 h, including the LPS sample introduction for 0.5 h, BP anchoring for 1 h, and the generation and amplification of the detection signal for less than 2 h, indicating great promise for on-site rapid analysis. Because of

its outstanding sensitivity and selectivity, visualization and rapidity, we anticipate that this analytical method could open up new opportunities for LPS detection in future clinical diagnosis, food security and environment monitoring.

Acknowledgments

This work was supported by National Natural Science Foundation Project of China (31671922) and Beijing Nova Program (No. xx2014B069).

Supporting Information

The tables of the DNA sequences used in this work, the analytical performance of other reported LPS detection methods and LPS analysis in real samples.

Notes

The authors declare no competing financial interest.

References

Beyer, S., Dittmer, W.U., Simmel, F.C., 2005. Journal of Biomedical Nanotechnology 1(1), 96-101.

Bouças, R.I., Trindade, E.S., Tersariol, I.L., Dietrich, C.P., Nader, H.B., 2008. Anal. Chim. Acta 618(2), 218-226.

Ding, S.-J., Chang, B.-W., Wu, C.-C., Chen, C.-J., Chang, H.-C., 2007. Electrochemistry communications 9(5), 1206-1211.

Dohno, C., Nakatani, K., Saito, I., 2002. Journal of the American Chemical Society 124(49), 14580-14585.

Ellington, A.D., Szostak, J.W., 1990. nature 346(6287), 818-822.

Filippov, N., Lomzov, A., Pyshnyi, D., 2009. Biophysics 54(3), 280-290.

Foto, M., Plett, J., Berghout, J., Miller, J.D., 2004. Analytical and bioanalytical chemistry 379(1), 156-162.

Gutsmann, T., Schromm, A.B., Brandenburg, K., 2007. International journal of medical microbiology 297(5), 341-352.

Hamaguchi, N., Ellington, A., Stanton, M., 2001. Analytical biochemistry 294(2), 126-131.

Jhaveri, S., Rajendran, M., Ellington, A.D., 2000. Nature biotechnology 18(12), 1293-1297.

Karympalis, V., Kalopita, K., Zarros, A., Carageorgiou, H., 2004. Biochemistry (Moscow) 69(8), 855-860.

Kim, S.-E., Su, W., Cho, M., Lee, Y., Choe, W.-S., 2012. Analytical biochemistry 424(1), 12-20.

Kim, Y.-G., Lee, C.-S., Chung, W.-J., Kim, E.-m., Shin, D.-S., Rhim, J.-H., Lee, Y.-S., Kim, B.-G., Chung, J., 2005. Biochemical and biophysical research communications 329(1), 312-317.

Kittelberger, R., Hilbink, F., 1993. Journal of biochemical and biophysical methods 26(1), 81-86.

Kotani, S., Takada, H., Tsujimoto, M., Ogawa, T., Takahashi, I., Ikeda, T., Otsuka, K., Shimauchi, H., Kasai, N., Mashimo, J., 1985. Infection and immunity 49(1), 225-237.

Lee, G.U., Kidwell, D.A., Colton, R.J., 1994. Langmuir 10(2), 354-357.

Lei, M., Morrison, D., 1988. The Journal of Immunology 141(3), 996-1005.

Li, D., Shlyahovsky, B., Elbaz, J., Willner, I., 2007. Journal of the American Chemical Society 129(18), 5804-5805.

Li, J., Purves, R.W., Richards, J.C., 2004. Analytical chemistry 76(16), 4676-4683.

Li, J.J., Fang, X., Tan, W., 2002. Biochemical and biophysical research communications 292(1), 31-40.

Li, N., Ho, C.-M., 2008. Journal of the American Chemical Society 130(8), 2380-2381.

Liu, J., Cao, Z., Lu, Y., 2009. Chemical reviews 109(5), 1948-1998.

Liu, J.R., Chen, G.F., Shih, H.N., Kuo, P.C., 2008. Phytomedicine 15(1-2), 23-30.

Macdougall, D., Crummett, W.B., 1980. Analytical Chemistry 52(14), 2242-2249.

Murai, T., Ogawa, Y., Kawasaki, H., Kanoh, S., 1987. Infection and immunity 55(10), 2456-2460.

Nutiu, R., Li, Y., 2003. Journal of the American Chemical Society 125(16), 4771-4778.

Pedersen, M., Hansen, E., Christensen, J., 1994. Journal of clinical pharmacy and therapeutics 19(3), 189-194.

Plum, G.E., 1997. Biopolymers 44(3), 241-256.

Rapson, N., 1988. Current Opinion in Infectious Diseases 1(6), 919-925.

Shen, Z.-Q., Wang, J.-F., Qiu, Z.-G., Jin, M., Wang, X.-W., Chen, Z.-L., Li, J.-W., Cao, F.-H., 2011. Biosensors and bioelectronics 26(7), 3376-3381.

Simoons-Smit, I.M., Appelmelk, B.J., Verboom, T., Negrini, R., Penner, J.L., Aspinall, G.O., Moran, A.P., Fei, S.F., Shi, B., Rudnica, W., 1996. Journal of clinical microbiology 34(9), 2196-2200.

Su, W., Lin, M., Lee, H., Cho, M., Choe, W.-S., Lee, Y., 2012. Biosensors and Bioelectronics 32(1), 32-36.

Tang, J., Hou, L., Tang, D., Zhang, B., Zhou, J., Chen, G., 2012. Chemical Communications 48(66), 8180-8182.

Tang, Z., Mallikaratchy, P., Yang, R., Kim, Y., Zhu, Z., Wang, H., Tan, W., 2008. Journal of the American Chemical Society 130(34), 11268-11269.

Therisod, H., Labas, V., Caroff, M., 2001. Analytical chemistry 73(16), 3804-3807.

Tuerk, C., Gold, L., 1990. Science 249(4968), 505-510.

Weber, P.C., Ohlendorf, D., Wendoloski, J., Salemme, F., 1989. Science 243(4887), 85.

Wilde, C., Schmidt, G., Moellenhoff, E., Chatterjee, B., Nakatani, S., Tsuda, T., Yamasaki, Y., Moriyama, H., Watanabe, H., Kato, Y., 2003. LC GC EUROPE, 17-19.

Xie, S., Dong, Y., Yuan, Y., Chai, Y., Yuan, R., 2016. Analytical chemistry 88(10), 5218-5224.

Zheng, J., Hu, Y., Bai, J., Ma, C., Li, J., Li, Y., Shi, M., Tan, W., Yang, R., 2014. Analytical chemistry 86(4), 2205-2212.

Zheng, J., Li, J., Jiang, Y., Jin, J., Wang, K., Yang, R., Tan, W., 2011. Analytical chemistry 83(17), 6586-6592.

Zhu, Z.X., Cong, W.T., Ni, M.W., Wang, X., Ma, W.D., Ye, W.J., Jin, L.T., Li, X.K., 2012. Electrophoresis 33(7), 1220-1223.

Fig. 1 Schematic of the design of the rapid and visual aptasensor for LPS detection based on the BTTS as a selective molecular recognition and signal transduction element and HCR-HRP nanostructures as effective signal amplifier and signal report element.

Fig. 2 Optimization of the immobilized CP. (A) OD_{450} of the BTTS aptasensor with different concentrations of SA (μg/mL). (B) OD_{450} of the BTTS aptasensor with different concentrations of CP (nM). Error bars represent the standard deviation (N = 3).

Fig. 3 Optimization of the BTTS aptasensor. (A) OD_{450} of the BTTS aptasensor with different lengths of flanked mirror sequences of BLA. a to h represent BLA1-BLA4 before and after the addition of LPS, respectively. (B) OD_{450} of the BTTS aptasensor with different pH of working buffer. a to h represent pH 5.0, 6.0, 7.0, 8.0 before and after the addition of LPS, respectively. (C) OD_{450} of the BTTS aptasensor with different ratios of BLA versus BP. a to h represented the ratios 0.9, 1.0, 1.1, and 1.2 before and after the addition of LPS, respectively. Error bars represent the standard deviation (N = 3).

Fig. 4 Characterization of the chromatographic behavior of the BTTS on a DNA-NPR

column. Fig. 4A, Fig. 4B and Fig. 4C present typical elution profiles of the negative control of the BLA3 and the BTTS composed of BLA3 and BP before and after the addition of LPS, respectively.

Fig. 5 Characterization of HCR-HRP nanostructures. (A) EB-stained agarose gel electrophoresis demonstrated BP-initiated HCR: lane 1, 2000-bp marker from top to bottom was 2000, 1000, 750, 500, 250, and 100 bp; Lane 2, 1.0 μM Biotin-H_1; Lane 3, 1.0 μM Biotin-H_2; Lane 4, mixture of 1.0 μM Biotin-H_1 and Biotin-H_2; Lanes 5-10, the presence of BP (100 nM, 150 nM, 200 nM, 400 nM, 500 nM, and 600 nM) with a mixture of Biotin-H_1 and Biotin-H_2. HCR time: 1 h. (B) OD_{450} of the BTTS aptasensor with different concentrations of SA-HRP (ng/mL). Error bars represent the standard deviation (N = 3).

Fig. 6 Analytical performance of the BTTS aptasensor for LPS detection. (A) Calibration plot of optical density vs. LPS detection. The dotted line represents the linear fit to the data. The inset shows semi- quantitatively color chart (upper) and chromogenic signal output (middle), the concentrations from left are 1, 10, 20, 50, 100 and 150 ng/mL of LPS. (B) Specificity of the BTTS aptasensor toward (a) blank control, (b) 50 ng/mL D-mannose, (c) 50 ng/mL BSA, (d) 50 ng/mL peptidoglycan from *S. aureus*, (e) 50 ng/mL Hb, (f) 50 ng/mL glucose, (g) 50 ng/mL HAS, (h) 50 ng/mL LPS from *E.coli O55:B5*, (i) 50 ng/mL D-mannose + 50 ng/mL BSA + 50 ng/mL peptidoglycan from *S. aureus* + 50 ng/mL Hb + 50 ng/mL glucose + 50 ng/mL HAS + 50

ng/mL LPS from *E.coli O55:B5* + 50 ng/mL LPS from *E.coli O111:B4*, (j) 50 ng/mL LPS from *E. coli O111:B4*. Error bars represent the standard deviation (N = 3).

Highlights

- A turn-on sensor for the detection of lipopolysaccharides based on a bulb-like triplex turn-on switch (BTTS) was developed.
- The visual sensor is based on HCR-HRP nanostructures.
- The sensor has a linear calibration of 1 ng/mL to 150 ng/mL.
- The on-site sensor can be used independent of sophisticated apparatus and has a reaction time less than 4h.
- The aptasensor displayed high selectivity and anti-interference.